

Supplementary Materials

Carbon Quantum Dot-Gold Nanoparticle System as Probe for Inhibition and Reactivation of Acetylcholinesterase: Detection of Pesticides

Jyoti Korram^a, Lakshita Dewangan^a, Rekha Nagwanshi^b, Indrapal Karbhal^a, Kallol K. Ghosh^a,
and Manmohan L. Satnami^{a*}

^aSchool of Studies in Chemistry, Pt. Ravishankar Shukla University, Raipur, 492 010,
Chhattisgarh India

^bDepartment of Chemistry, Govt. Madhav P.G. Science College, Ujjain, Madhya Pradesh, India
manmohanchem@gmail.com

Materials and Instruments

All the reagents used were purchased from Sigma-Aldrich, Bengaluru (India). Hydrogen tetrachloroaurate (III) hydrate, AChE (500 U/mL from *Electrophorus electricus* (electric eel)), acetylthiocholine iodide (ATChI), paraoxon, malathion, methamidophos, carbaryl, trisodiumcitratetridihydrated and citric acid were. Quaternizedoxime (1-dodecyl-4-((hydroxyimino) methyl) pyridinium bromide (4-C₁₂PyOx⁺) was synthesized by previously reported method.¹ All the experiments were performed using Milli-Q ultrapure water and the reagents used were of analytical grade. The FL spectra were collected with an Agilent Eclipse fluorescence spectrophotometer (G9800AA). UV-visible spectra recorded using Thermo Scientific Evolution 300 spectrophotometer. Dynamic light scattering (DLS) and zeta potential measurements were performed on a zeta sizer nano ZS. Transmission electron microscopy (TEM) and high-resolution TEM (HRTEM) images were measured with a transmission electron microscope (NCL Pune,

India). Time resolved fluorescence measurements were carried out using time-correlated single photon counting (TCSPC) spectrometer (Delta Flex-01-DD/HORIBA).

Preparation of citrate-capped AuNPs

AuNPs were synthesized through the reduction of HAuCl₄ by sodium citrate. Briefly, trisodium citrate solution (38.8 mM L⁻¹, 5.0 mL) was added to boiling HAuCl₄ (1 mM L⁻¹, 50 mL) solution under continuous magnetic stirring. After the colour of the solution changed from yellow to red wine, the mixture was refluxed for 10 min before cooled down to room temperature. The molar extinction coefficient (ϵ) of the AuNPs at 520 nm is about $2.7 \times 10^8 \text{ M}^{-1} \text{ cm}^{-1}$. The final concentration was calculated to be 4.2 nML⁻¹ according to Lambert Beer's law.

Quantum yield (QY) measurement

The quantum yield (QY) of CQDs was obtained by the following equation 1:

$$Q = Q_s \frac{Y I_s \eta^2}{Y_s I \eta_s^2} \quad (1)$$

Where Q is the QY, Y is the optical density, I is the measured integrated emission intensity, and η is the refractive index of the solvent. The subscript “s” refers to the standard with known QY. For these aqueous solutions, $\eta/\eta_s=1$. Quinine sulfate (0.1 M, H₂SO₄ as solvent; QY= 0.54%) were chosen as standards 2 (Figure S1). The relative quantum yield of CQD found to be 5.33%.

Specificity of investigation

The feasibility of the above method was tested by performing the analysis using spiked tap water, river water and apple juice. Aliquots of the different concentration (0.3 ng mL⁻¹, 0.6 ng mL⁻¹ and 1.8 ng mL⁻¹) of OPs, prepared by diluting stock solutions were mixed with AChE

(20 ng mL⁻¹) and incubated for 30 min. The mixture was further incubated for 15 min after the addition of ATChI (1mM) and CQD/AuNPs followed by the FL measurements. Pesticide residues were then determined using the standard correlation curve.

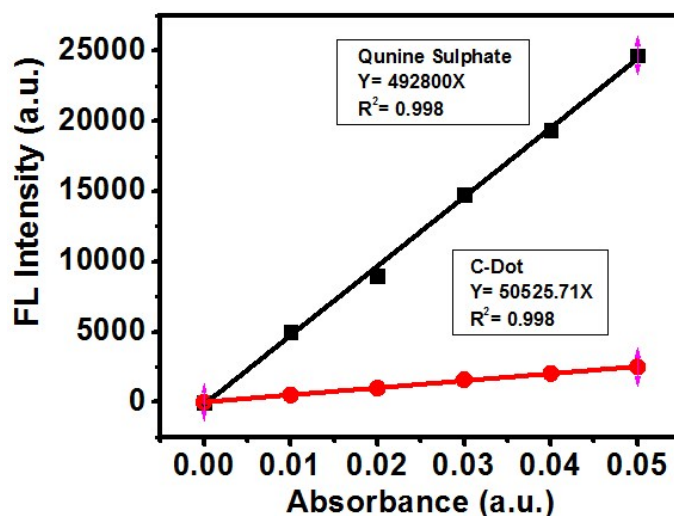


Figure S-1 Calibration curve between absorbance (360 nm) and FL intensity (490 nm) for the determination of relative quantum yield of CQD.

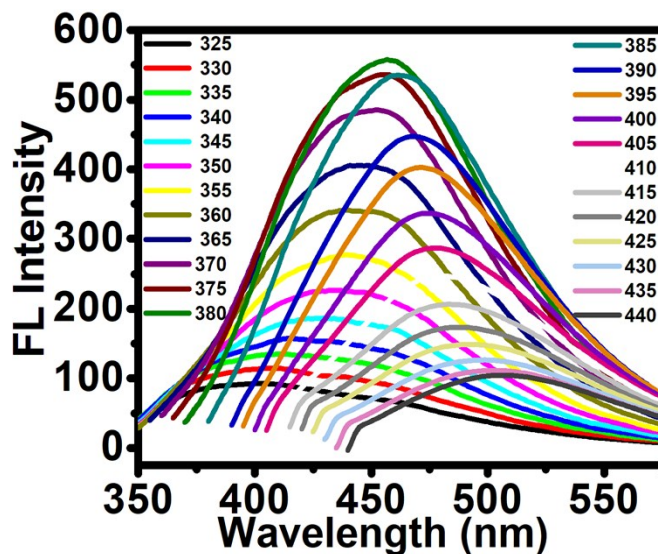


Figure S-2 FL intensity with the different excitation from 325 nm to 440 nm of CQD.

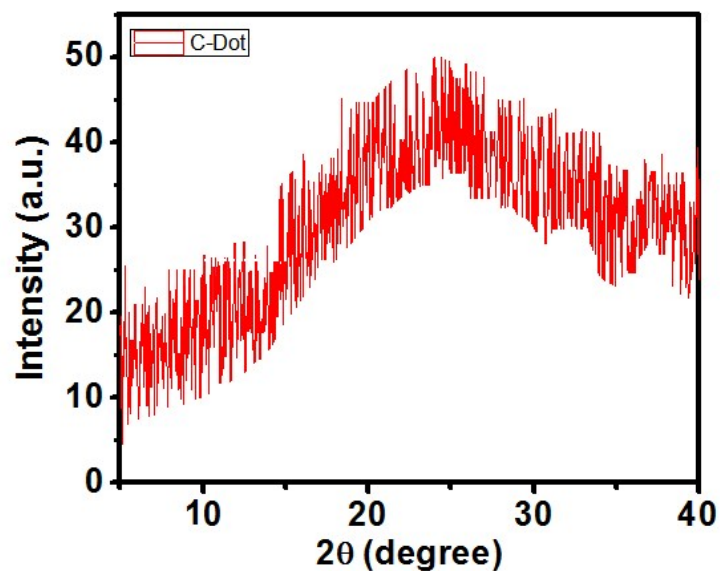


Figure S-3 The XRD spectra of CQD.

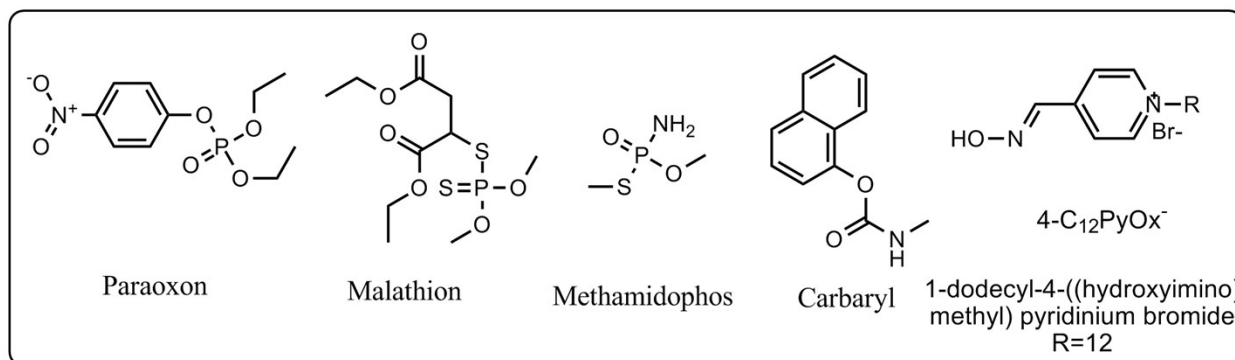


Chart S-1 Shows the chemical structure of OPs and carbamate and Oxime.

Fluorescence quenching of CQD by AuNPs

In order to investigate FRET based FL quenching of CQD, some important experimental parameters are optimized: (a) amount of CQDs; (b) pH value of phosphate buffer; (c) reaction time (d) effect of temperature etc. (Figure S4). The following optimal experimental conditions were found to give best results: (a) amount of CQDs of 0.47 mg mL^{-1} ; (b) pH value of 8.0; (c) reaction time of 16 min. The FL intensity of CQDs was quenched as function of different concentration of AuNPs in the range of 0-2.60 nM without any peak position shift when AuNPs was present (Figure 4a). Furthermore, the FL quenching of CQDs by AuNPs can be described by the following Stern-Volmer equation:

$$I_0 - I_A / I_A = K_{SV} * [Q] \quad (6)$$

Where K_{SV} is the Stern-Volmer quenching constant, $[Q]$ is the concentration of AuNPs, I_0 and I_A represent the FL intensity of CQDs in the absence and presence of AuNPs, respectively. The relative FL intensity of CQDs exhibited a good linear relationship with the concentration of AuNPs in the range of 0 to 2.60 nM (Figure 4c). A calibration curve of $(I_0 - I_A) / I_A = 3.0 \times 10^8 \text{ M} \times [\text{AuNPs}]$ was obtained with a correlation coefficient of 0.9949 and a standard deviation of 1.87%. From the slope of the linear plot, the Stern-Volmer quenching constant K_{sv} was calculated to be $3.0 \times 10^8 \text{ M}$. The relative standard deviation for 0.62 nM AuNPs was 0.2% ($n = 6$), indicating the high precision of CQDs fluorescent probe, (Figure 4b).

Table S1: Fluorescence decay parameter for CQD and CQD-Au ($\lambda_{ex} = 380$ nm and $\lambda_{em} = 468$ nm); the decay times (τ_1 , τ_2 and τ_3) and the respective functional contributions (α_1 , α_2 and α_3), the weighted average decay time (τ_{av}) and the quality of fitting (χ^2) are shown.

Sample	$\lambda_{em}(nm)$	τ_1 (ns)	α_1 %	τ_2 (ns)	α_2 %	τ_3 (ns)	α_3 %	χ^2	$\tau_{av}(ns)$
CQD	468	1.5	47	5.3	45	0.2	8	1.10	3.10
CQD-Au	468	1.3	75	4.3	25	---	---	1.04	2.0

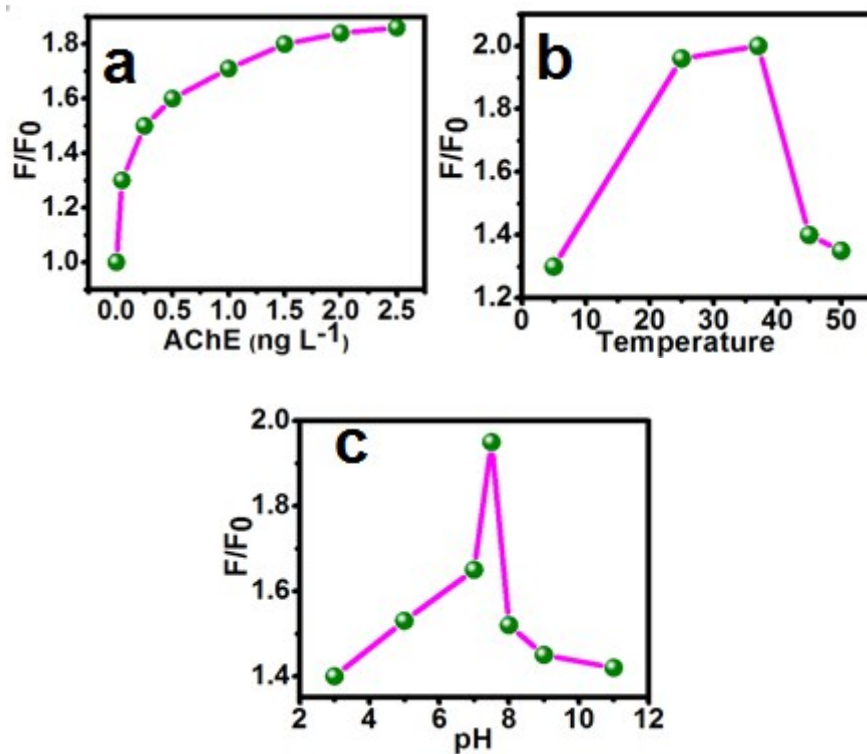


Figure S-4 The effect of the concentrations of AuNPs (a), the pH of the solution (b), incubation temperature (c) the recovery percentages of FRET based fluorescence sensing platform.

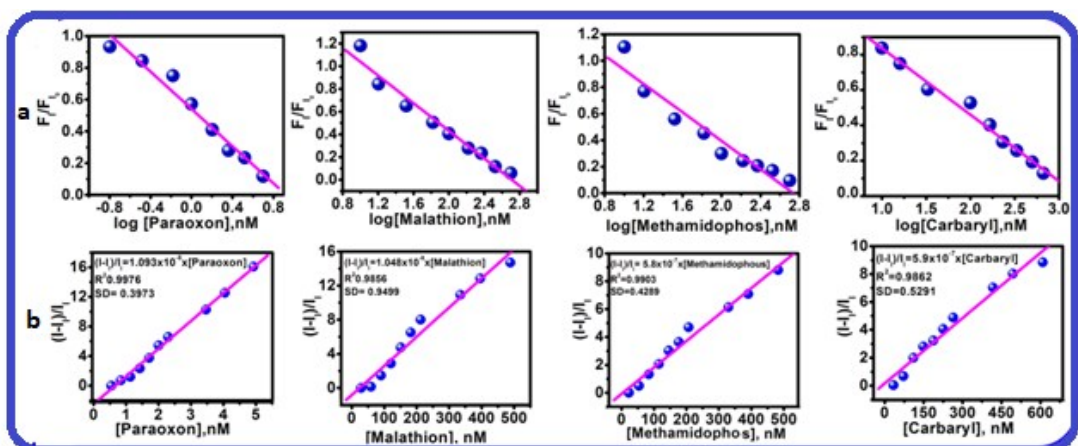


Figure S-5 (a) The calibration curve between logarithm concentration of pesticides and F_1/F_{10} , (b) the linear calibration curve between pesticides concentration and Ksv.



Figure S-6 Photographical image of CQD with the increasing concentration of 4-C₁₂-PyOx⁻ (oxime) in cocktail of AuNPs, ATChI, AChE and paraoxon.

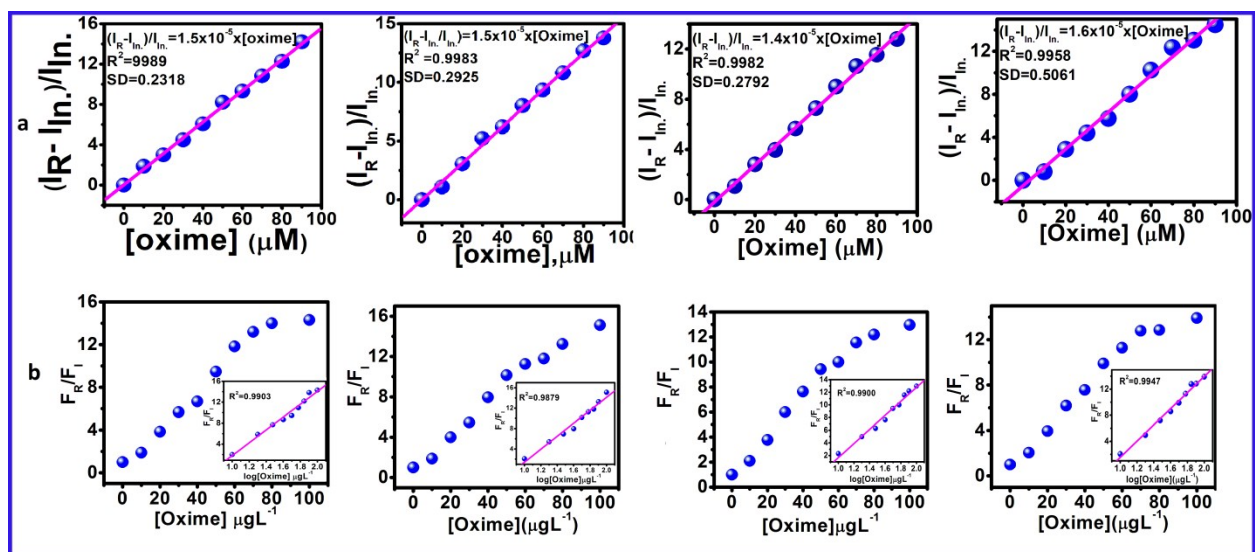


Figure S-7 (a) The relationship between K_{sv} and concentration of oxime, (b) The calibration curve of F_R/F_I and concentration of oxime. inset; The linear calibration curve of F_R/F_I and logarithm concentration of oxime.

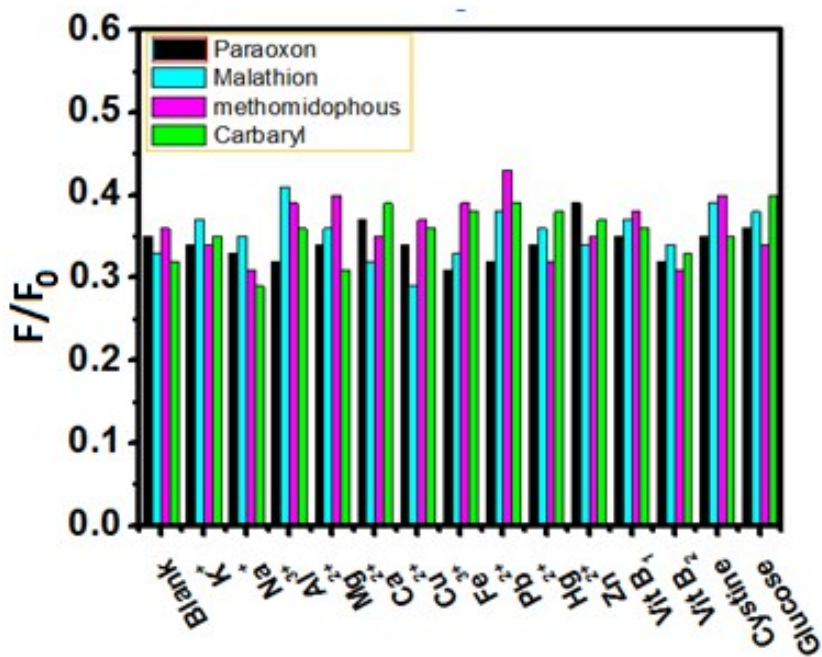


Figure S-8. Bar graph displayed the calibration of FL intensities at 490 nm of CQD-AuNPs–AChE–ATCh in the presence of 30 ng mL⁻¹ paraoxon, malathion, methamidophos, carbaryl vs. premixed with different interferences i.e. F/F₀. The columns represent the FL intensities at 490 nm of a control sample with different interfering substances: Na⁺(0.13 mg mL⁻¹), K⁺(0.10 mg mL⁻¹), Mg²⁺(0.14 mg mL⁻¹), Ca²⁺(0.17 mg mL⁻¹), Fe³⁺(1.5 µg mL⁻¹), Pb²⁺(0.22 mg mL⁻¹), Hg²⁺(0.32 mg mL⁻¹), Zn²⁺(0.019 mg mL⁻¹) cysteine (2.0 µg mL⁻¹), glucose (3.2 µg mL⁻¹), vitamin B₁ (5.0 µg mL⁻¹), and vitamin B₂ (3.1 µg mL⁻¹) respectively.

Table S-2 Comparison of the proposed method with other methods based on the AChE for detection of paraoxon.

Method	Linear range	LOD	References
Fluorescence Sensor	10-250 nM	5×10^{-6} µM	2
Luminescence	-	1.05×10^{-5} µM	3
Amperometric	1 nM - 5 µM	0.7 nM	4
Colorimetric Detection	0.30 -17.30 ng mL ⁻¹	0.13 ng mL ⁻¹	1
Conductometric	-	10^{-6} M	5
Cyclic Voltametry	0.5 - 40 µM	0.5 µM	6
Fluorescence Sensor	0.16 - 5 nM	5×10^{-2} nM	This work

Table S-3 Comparison of the proposed method with other methods based on the AChE for detection of malathion.

Method	Linear range	LOD	References
Electrochemical	-	0.1 nM	7

Colorimetric	-	60 ng mL ⁻¹	8
Amperometric	-	3.3 nM	9
Differential Pulse Voltammetry	-	0.3 nM	10
Differential Pulse Voltammetry	0.07–1.3 ppm	0.18 nM	11
Fluorescence	10-500 nM	0.1 nM	This work

Table S-4 Comparison table of the proposed method with other methods based on the AChE for methamidophos detection.

Method	Linear range	LOD	References
Amperometric	0.1 - 100 μM	3.8 nM	12
Fluorescence	3.50×10^{-7} – 0.71×10^{-3} ML ⁻¹	9.16×10^{-8} M	13
Colorimetric	0.02–1.42 μg mL ⁻¹	1.40 ng mL ⁻¹ .	14
Potentiometric	-	10 ng L ⁻¹	15
Mass-Specrometry	1.01–9.33 ng mL ⁻¹	1.97 ng mL ⁻¹	16
Liquid Chromatographic Tandem Mass Spectroscopic	5 to 50 μg L ⁻¹	2 μg L ⁻¹	17
Fluorescence	10-500 nM	0.12 nM	This work

Table S-5 Comparison between proposed and other methods based on the AChE activity in terms of carbaryl detection.

Method	Linear range	LOD	References
Raman Spectroscopy	0-10 $\mu\text{g L}^{-1}$	0.5 mg g^{-1}	18
Colorimetric	1×10^{-6} - 1×10^{-4} g L^{-1}	0.007 $\mu\text{g L}^{-1}$	19
Electrochemical	1.0×10^{-7} - 1.0×10^{-4} M L^{-1}	8.0×10^{-8} M L^{-1}	20
Electrochemical	2.58×10^{-7} - 2.58×10^{-2} $\mu\text{g mL}^{-1}$.	10^{-8} $\mu\text{g mL}^{-1}$	21
Amperometric	9.9×10^{-3} - 9.93 μM	3.4×10^{-3} μM	22
Fluoremetric	1×10^{-8} - 1×10^{-4} gL^{-1}	0.006 $\mu\text{g L}^{-1}$	23
Piezoelectric	1×10^{-7} - 5×10^{-5} M	1.0×10^{-7} M	24
Squarewave Voltammetry	9.90×10^{-8} - 2.91×10^{-8} M	1.98×10^{-8} M	25
Differential Pulse Voltammetry	0.5–200 μM	7.5 $\mu\text{g L}^{-1}$	26
Fluorescence	10 - 666 nM	0.13 nM	This work

Table S-6 Reactivation parameter of oxime induced reactivation of pesticides-inhibited AChE.

Pesticides	K_D μM	K_r (min⁻¹)	K_{r2} nM min⁻¹	% R
Paraoxon	12.61± 4.358	1.149±0.074	0.072± 0.018	98.91%,
Malathion	15.88± 3.909	1.221±0.097	0.096± 0.022	90.73%,
Methamidophos	43.36 ± 11.50	1.568±0.174	0.036± 0.015	80.91%
Carbaryl	48.81 ± 12.26	1.612±0.178	0.033± 0.014	83.91%

Table S-7 Detection of Organophosphorus and Carbamates pesticides in spiked real samples

Real samples	Spiked (ng mL ⁻¹)	Paraoxon			Malathion			Methamidophos			Carbaryl		
		FOUND (ng mL ⁻¹)	RECOVERY (%)	RSD (%) (n=6)	FOUND (ng mL ⁻¹)	RECOVERY (%)	RSD (%) (n=6)	FOUND (ng mL ⁻¹)	RECOVERY (%)	RSD (%) (n=6)	FOUND (ng mL ⁻¹)	RECOVERY (%)	RSD (%) (n=6)
River water	0.3	0.23	110.3	3.03	0.29	96.6	3.44	0.30	100	3.33	0.33	110	2.72
	0.6	0.58	96.6	6.06	0.61	101.6	1.63	0.56	93.3	1.60	0.56	93.3	1.60
	1.2	0.98	98.2	4.02	1.10	98.01	2.21	0.96	102.2	2.56	0.99	96.5	3.84
Tap water	0.3	0.32	106.6	4.22	0.24	80.0	2.33	0.29	97.6	3.10	0.27	90.2	3.33
	0.6	0.57	95.4	3.91	0.57	95.0	1.75	0.58	96.6	1.55	0.52	86.6	1.90
	1.2	1.0	103.1	3.76	1.15	102.3	3.21	0.96	95.3	2.30	0.98	105.1	4.12
Apple Juice	0.3	0.26	106.6	7.69	0.28	93.3	3.57	0.29	99.1	3.44	0.25	83.0	3.60
	0.6	0.58	95.4	1.75	0.55	91.6	1.81	0.61	101.6	1.63	0.59	98.3	1.63
	1.2	0.99	107.1	4.02	1.02	98.01	3.21	0.96	92.2	2.56	0.99	96.5	4.81

References

1. M. L. Satnami, J. Korram, R. Nagwanshi, S. K. Vaishnav, I. Karbhal, H. K. Dewangan, K. K. Ghosh, *Sens. Actuators, B*, 2018, **267**, 155.
2. R. Khaksarinejad, A. Mohsenifar and R. T. Cherat, *Appl. Biochem. Biotechnol.* 2015, **176**, 359.
3. Z. Zheng, Y. Zhou, X. Li, S. Liu, Z. Tang, *Biosens. Bioelectron.* 2011, **26**, 3081.
4. Q. Lang, L. Han, C. Hou, F. Wang, A. Liu, *Talanta*, **156**, 2016, 34.
5. S. V. Dzydevich, A. A. Shul'ga, A. P. Soldatkin, A. M. N. Hendjz, N. J. Renault, C. Martele, *Electroanalysis*, 1994, **6**, 752.
6. Y. Zhang, M. A. Arugula, M. Wales, J. Wild, A. L. Simonian, *Biosens. Bioelectron.* 2015, **67**, 287.
7. M. H. M. Facure, L. A. Mercante, L. H. C. Mattoso, D. S. Corre, *Talanta*, 2017, **167**, 59.
8. S. Singh, P. Tripathi, N. Kumar, S. Nara, *Biosens. Bioelectron.* 2017, **15**, 280.
9. M. Amatatongchai, W. Sroysee, P. Jarujamrus, P. A. Lieberzeit, *Talanta*, 2018, **179**, 700.
10. D. Huo, Q. Lia, Y. Zhang, C. Houa, Y. Lei, *Sens. Actuators, B*, 2014, **199**, 410.
11. P. Raghu, T. M. Reddy, K. Reddaiah, B. E. K. Swamy, M. Sreedhar, *Food Chem.* 2014, **142**, 188.
12. D. Du, X. Ye, J. Cai, J. Liu, A. Zhang, *Biosens. Bioelectron.* 2010, **25**, 2503.
13. X. Liu, Q. Liu, F. Kong, X. Qiao, Z. Xu, *Adv. Poly. Tech.* 2017, **90**, 1.
14. H. Li, J. Guo, H. Ping, L. Liu, M. Zhang, F. Guan, C. Sun, Q. Zhang, *Talanta*, 2011, **87**, 93.
15. B. Rajangam, D. K. Daniel, A. I. Krastanov, *Eng. Life Sci.* 2018, **18**, 4.
16. M. A. Montesano, A. O. Olsson, P. Kuklenyik, L. L. Needham, A. S. Bradman, D. B.

- Barr, *J. Exposer Sci. Environ. Epidemiol.* **17**, 2007, 321.
17. V. Kumar, N. Upadhyay, V. Kumar, S. Sharma, *Arabian J. Chem.*, 2015, **8**, 624.
 18. Y. Fan, K. Lai, B. A. Rasco, Y. Huang, *LWT Food Sci. Technol.* 2015, **60**, 352.
 19. D. Zhao, C. Chen, J. Sun, X. Yang, *Analyst*, 2016, **141**, 3280.
 20. M. Sergi, M. D. Carlo, A. Pepe, D. Compagn, *Talanta*, 2018, **186**, 389.
 21. C. T. Thanh, N. H. Binh, N. V. Tu, T.V. Thu, M. Bayle, Paillet, J. L. Sauvajol, Thang, T. D. Lam, P. N. Minh, N. V. Chuc, *Sens. Actuators, B* 2018, **260**,78.
 22. K. Wang, Q. Liu, L. Dai, J. Yan, C. Ju, B. Qiu, X. Wu, *Anal. Chim. Acta*, 2011, **695**, 84.
 23. C. J. Murphy, *Anal. Chem.* 2002, **74**, 520A.
 24. J. M. Abad, F. Pariente, L. Herna´ndez, H. D. Abrun, E. Lorenz, *Anal. Chem.*, 1998, **70**, 2848.
 25. M. B. F. Thiago, M. Oliveira, F. Barroso, S. Morais, M. Araújo, C. Freire, P. Lima-Neto, A. N. Correia, M. B.P.P. Oliveira, C. Delerue-Matos. *Bioelectrochemistry*, 2014, **98**, 20.
 26. M.Y. Wang, J. R. Huang, M. Wang, D. E. Zhang, J. Chen, *Food Chem.* 2014, **151**, 191.